ISSN 2347-3487

LPG sensing investigation of (Sn-Ti)O_2 system based nanocomposite at Room Temperature

Tripti Shukla* and S.K. Omanwar
Department of Physics,
Sant Gadge Baba Amravati University Amravati-444602, M.S., India
*Email: triptishukla.20@rediffmail.com

Abstract

Present work reports the synthesis of pure TiO_2 and (Sn-Ti)O_2 nanocomposite, its characterization and performance as Liquefied Petroleum Gas (LPG) Sensor. Thick films of both the materials were prepared by using screen printing technique. After that these were investigated through SEM. SEM image of pure TiO_2 shows that grains are random in shape having pores. The grains observed on the (Sn-Ti)O_2 thick-film surface are spherical in shape and more porous than pure TiO_2. Further at room temperature, the films were exposed to LPG in a controlled gas chamber and variations in resistance with the concentrations of LPG were observed. The maximum value of average sensitivity for pure TiO_2 and (Sn-Ti)O_2 thick-film were found 3.0 and 11 respectively for 2 vol.% of LPG. Sensor responses as a function of exposure and response times were also estimated and maximum sensor response for pure TiO_2 and (Sn-Ti)O_2 thick-film were found 207 and 1040 respectively.

Key Words

LPG Sensor, nanocomposites, sensitivity, SEM and XRD.

Council for Innovative Research
Peer Review Research Publishing System
Journal: JOURNAL OF ADVANCES IN PHYSICS
Vol. 11, No. 5
www.cirjap.com, japeditor@gmail.com

ISSN 2347-3487

Introduction

The increasing concerns with pollution on health and safety stress the need of monitoring all aspects of the environment in real time, and in turn led to a tremendous effort in terms of research and funding for the development of sensors devoted to several applications [1–3]. Gas sensors are used widely in industry, in households and in a variety of other locations to monitor various gases and vapors [4-8]. The development of gas sensors to monitor combustible gases is imperative due to the concern for safety requirements in homes and for industries, particularly LPG. Because LPG is a flammable gas which presents many hazards to both the humans and an environment. Due to its highly flammable characteristics, even low level concentration (ppm) poses a serious threat. With the global population boom, more and more human lives are being endangered by the effect of LPG exposure. LPG is used as an automotive fuel or as a propellant for aerosols, in addition to other specialist applications. The widespread use of LPG for cooking and as fuel for automobile vehicles requires fast and selective detection of LPG to precisely measure the leakage of gas for preventing the occurrence of accidental explosions. In spite of considerable efforts, good sensor for LPG has not been found hitherto, the problem being of vital significance to industry as well as general public [9-14]. Therefore the detection of LPG is necessary for domestic appliances at low concentration level. Gas sensors employ different types of materials. Metal-oxide-semiconductor (MOS) sensors are very promising due to their high sensitivity, small dimensions, low cost, and good compatibility with the fabrication process for microelectronic devices. Besides bulk oxides, nanostructured metal oxide semiconductors have been employed as gas sensors. The metal oxides such as SnO_2 [15], ZnO [16], Fe_2O_3 [17] and TiO_2 [18] offer the potential for developing a portable and inexpensive gas sensing devices, which have the advantages of simplicity, high sensitivity and fast response. They operate on the basis of the modification of electrical conductivity of metal oxide layers, resulting from the interactions between ionosorbed moieties such as O_2^-, O−, and O^{2-} species and gas molecules to be detected.

In order to obtain a LPG sensor with outstanding performance, the recent research works were committed to nanocomposite because they have large surface area and contain more grain boundaries. Nanocomposites have recently emerged as promising candidates for gas detection. It has been realized that such systems may benefit from the combination of the best sensing properties of the pure components. It has been shown that simple metal oxides could not fulfill all the demands to make a perfect gas sensing matrix. Therefore to overcome this imperfection, its sensing capability has been improved with the other metal oxide additives to complex multicomponent materials [19–24]. Formation of mixed oxides leads to the modification of the electronic structure of the system. This includes the changes in the bulk as well as in the surface properties. Bulk electronic structure, the band gap, Fermi level position, transport properties, and so forth are affected mostly in the case of compounds and solid solutions. Surface properties are expected to be influenced by new boundaries between grains of different chemical compositions. It is anticipated that all these phenomena will contribute advantageously to the gas sensing mechanism. These additives enhance sensitivity of the sensor and improvement of their selectivity, decrease the response and recovery time, stabilize a particular valence state and favor the formation of active phases or increase the electron acceptor rate. From the general point of view, TiO_2 doping in pure SnO_2 is thought to modify the microstructure of the base material, to control grain growth mechanism and to introduce electronic states at the surface or into the bulk of the grain giving change to a modification of the base material conductivity and of the gas sensing properties [25-28].

In the present investigation we have synthesized (Sn-Ti)O_2 nanocomposite through soft chemical route. Furthermore, the as-prepared samples were used to fabricate into sensing elements by using screen printing technique. In fact, screen-printing is a simple and automated manufacturing technique that allows the production of low cost and robust chemical sensors with good reproducibility. Such technique allows the deposition of a controlled amount of paste with a thickness ranging between few micrometer and some tens of micrometer. After that, we investigated their sensing performance towards Liquefied Petroleum Gas at room temperature for different concentration of LPG.

Experimental details

Synthesis of SnO_2

SnO_2 was prepared by mechanochemical method. $SnCl_2.2H_2O$ is dissolved in distilled water with continuous stirring for 5-6 hrs. Ammonium hydroxide was mixed dropwise in the solution under continuous stirring. Further the solution was sonicated for 30 minutes using ultrasonic machine. The precipitate was washed repeatedly with distilled water. The as-prepared product is referred as hydrous SnO_2. The as-prepared hydrous SnO_2 was again washed with ethanol and further sonicated in ethanol for 30 minutes.

$SrCO_3$ nanoparticles were prepared by dropping NH_4HCO_3 solution into 0.05M $Sr(NO_3)_2$ and they were stirred continuously for 2 hrs. Further, this solution was sonicated for 30 minutes and then washed with ethanol. The $SrCO_3$ nanoparticles were dissolved in ethanol and formed a suspension. This suspension was added to the ethanol treated hydrous SnO_2 suspension under stirring. 10% HNO_3 solution was added to this solution and further sonicated for 30 minutes. Finally HNO_3 solution was added to remove $SrCO_3$ particles. The mixture was evaporated on heating with stirring, dried at 120^{o}C and calcined at 600^{o}C for 2 hrs. The solid product at this stage was SnO_2 powder. The single step thermal decomposition was taken place. The equation of reaction is given as under:

ISSN 2347-3487

$$SnCl_2.2H_2O + NH_4OH \xrightarrow[60°C]{} SnO_2 + NH_4Cl \uparrow + 2H_2O \uparrow + HCl \uparrow$$

(powder)

Synthesis of TiO_2

Nanosized TiO_2 was synthesized using an aqueous $TiCl_3$ solution and heated at 648 K.

Chemical reaction taking place is given below:

$$2TiCl_3 + 4H_2O \rightarrow 2TiO_2 + 4H_2 \uparrow + 3Cl_2 \uparrow$$

A white colored TiO_2 powder was obtained.

Synthesis of (Sn-Ti)O_2 Nanocomposite

SnO_2 was prepared by mechanochemical method and TiO_2 was prepared through hydrolysis of $TiCl_3$. Thereafter TiO_2 powder was evenly mixed with SnO_2 powder by weight 50% within an ethanol as solvent and stirred for 13 h. The solution was dried at 120 °C in an electric oven and further calcined at 450 °C for 1h; finally a white fine powder of (Sn-Ti)O_2 nanocomposite was obtained.

Preparation of thick film

A thick film of pure TiO_2 and (Sn-Ti)O_2 nanocomposite powders were prepared using following procedure. The thixotropic paste was formulated by mixing the resulting fine powder with a solution of ethyl cellulose (a temporary binder) in a mixture of organic solvents such as butyl carbitol acetate. The ratio of inorganic to organic part was kept as 75:25 in formulating the pastes. The thixotropic paste was screen printed on a glass substrate in desired patterns. The films prepared were fired at 500^0C for 1 h. Thus a thick film of pure TiO_2 and (Sn-Ti)O_2 nanocomposite were prepared.

These films were put within the Ag-film-Ag electrode configuration and exposed to LPG in a self-designed conventional chamber. Variations in resistance with the time after exposure were recorded by using Digital multimeter.

Characterization Technique

Scanning Electron Microscopy

The morphology of the sensing material for pure TiO_2 and (Sn-Ti)O_2 in the form of thick film were investigated with a scanning electron microscope at room temperature. Figure 1(a) shows the SEM of synthesized pure TiO_2 at nanoscale. It reveals that the particles are of spherical shape with uniform distribution having small pores. Figure 1(b) shows the SEM of (Sn-Ti)O_2 nanocomposite. It reveals that particles of (Sn-Ti)O_2 are random in shape having pores. These pores serve as gas adsorption sites and gas sensitivity depends on these pores. It is clearly shows that the surface of (Sn-Ti)O_2 thick film is more porous than the pure TiO_2 surface. A bunch like morphology has been disappeared in this figure and LPG interacts better with that type of morphology than Figure 1(a). Therefore the screen printed (Sn-Ti)O_2 film can adsorb atmospheric oxygen very easily and the amount adsorbed oxygen depends on the exposed surface area of the film. The grains observed on the surface are spherical in shape.

X-Ray Diffraction

X-Ray Diffraction pattern shown in Figure 2 obtained by X-Pert, PRO XRD system (Netherland) reveals crystalline nature of the sample. Figure 2(a) shows the XRD pattern of the pure TiO_2 powder. The high intensity peak centered at $2\theta = 25°$ is assigned to tetragonal TiO_2 with anatase phase (101) reflection having 'd' spacing 3.52182 Å and FWHM 0.0708°. Also the peak with low intensity at $2\theta = 44°$ assigned to TiO_2 (210) reflection having 'd' spacing 2.05772 Å and FWHM 0.3149° is assigned to rutile phase. The minimum crystallite size was found to be 17 nm at $2\theta = 68°$ with 'd' spacing 1.36472 Å and FWHM 0.5668°. Figure 2(b) shows that XRD pattern for (Sn-Ti)O_2 shows in that sample contains major phase of at the plane (211) for $2\theta = 52.25°$. The FWHM and d-spacing corresponding to this peak are 1.33° and 1.7507 Å respectively. The second intense peak of (Sn-Ti)O_2 for the plane (310) is at $2\theta = 62.67°$ with d-spacing and FWHM 1.4811 Å and 1° respectively. The XRD data thus confirms the formation of (Sn-Ti)O_2. The minimum crystallite size was found 7 nm at $2\theta = 52.25°$ with d-spacing and FWHM 1.7507 Å and 1.33° respectively.

UV-visible Spectroscopy

Optical characterization of the sensing material was done by using UV-Visible spectrophotometer (Varian, Carry-50 Bio). Figure 3(a) and 4(a) represent the variation of optical absorbance for the of pure TiO_2 and (Sn-Ti)O_2 in the form of thick film with the wavelength. The figures showed that absorbance decreases with increase in wavelength. In the UV region i.e. approximately in the range 4.0-3.5 eV, curves show steep decrease in absorbance. This data was further used for analyzing optical band gap energy (E_g) using the following formula for optical absorption of a semiconductor

ISSN 2347-3487

$$\alpha = \frac{K\left(h\nu - E_g\right)^{n/2}}{h\nu}$$

where α is the absorption coefficient, K is a constant, E_g the optical band gap of (Sn-Ti)O_2 thick film and n is an integer equal to 1 for a direct band gap and 4 for an indirect band gap.

Figure 3(b) and 4(b) show the Tauc plot of $(\alpha h\nu)^{1/2}$ versus photon energy ($h\nu$) for pure TiO_2 and (Sn-Ti)O_2 in the form of thick film. By extrapolating the linear part of the curve, the estimated value of the band gap was found to be 3.48 eV for pure TiO_2 and 3.90 eV for (Sn-Ti)O_2 nanocomposites. The higher band gap can be attributed to size and morphological effect of the present nanocomposites. Thus, the increase of band gap of (Sn-Ti)O_2 nanocomposites as compared to the pure TiO_2. This value of optical band gap shows blue shift, which is useful for LPG sensing applications. The higher band gap can be attributed to size and morphological effect and better sensing behavior of the nanocomposite

FTIR Analysis

The FTIR spectra of the sensing material were recorded at Perkin-Elmer Spectrum with ATR Accessory (ZnSe, Pike Miracle Accessory) and cadmium telluride (MCT) detector. Resolution was 4 cm^{-1} and 24 scans with 0.2 cm/s scan speed. Figure 5 shows the FTIR absorption spectra of (Sn-Ti)O_2 sample calcined at 450°C. The broad absorption peak observed in the region 500-800 cm^{-1} fall in the region corresponding to the vibrations of the type Ti-O-M (M = Sn), stretching and deformation modes respectively.

Activation Energy

The temperature - resistance plot in the form of ln R and (1000/T), known as Arrhenius plot, has a slope of (ΔE/2K) according to equation

$$\ln R = \ln R_o + \Delta E/2KT$$

Where ΔE, K and T are the activation energy, Boltzmann constant and absolute operating temperature respectively. The thick film of (Sn-Ti)O_2 was put inside a tubular furnace in the mid of the tube with electrical connections and variations in electrical resistance with temperature were recorded using a digital multimeter. Corresponding Arrhenius plot is shown in Figure 6. By measuring the slope of Arrhenius plot of a linear zone, we have calculated the activation energy of (Sn-Ti)O_2 and found 0.398 eV. This plot shows the variations of logarithmic resistance as a function of inverse temperature for the (Sn-Ti)O_2 nanocomposite. This establishes the semiconducting nature of material and it is due to the thermally activated mobility of the carriers rather than to a thermally activated generation of these.

Principle of Operation

Sensitivity is the measure of physical and/ or chemical properties of the sensing material when it is exposed by the desired gas. This term is also used to indicate either to the lowest level of chemical concentration or to the smallest increment of concentration that can be detected in the sensing environment. Greater is the change in physical properties of the sensing element under consideration, greater will be the sensitivity of the sensor. Here we have estimated resistance of the thick film as monitoring quantity and therefore the sensitivity of LPG sensor may be defined as the ratio of the resistance in presence of the LPG to the resistance in presence of the air, i.e.

$$S = \frac{R_g}{R_a}$$

The electrical resistances of the thick film in air (R_a) and in presence of LPG (R_g) were measured to evaluate the sensor response (SR) which is given as

$$\%SR = \frac{\left|R_a - R_g\right|}{R_a} * 100$$

Results and discussion

During experiment, each time exposing LPG to the pure TiO_2 and (Sn-Ti)O_2 thick film, it was allowed to equilibrate inside the gas chamber for 20-25 minutes and the stabilized resistance was taken as Ra. The variations in resistance with time after exposure for different concentrations of LPG were observed as shown in Figure 7 (a and b) for pure TiO_2 and (Sn-Ti)O_2 respectively. Figure 7 (a) illustrates variations in resistance of pure TiO_2 thick film with time after exposure for different vol.% of LPG at room temperature. Finally the outlet of the chamber was opened, the resistance approaches to their initial value of stabilized resistance in air (R_a) for further range of time. Curve R1 for 0.5 vol.% of LPG shows that the resistance increases from 82.73 MΩ to 128.82 MΩ after that it becomes constant. Curve R2 for 1 vol.% of LPG exhibits improvement over the previous and the resistance increases from 82.73 MΩ to 155.83 MΩ and then it becomes constant. Curve R3 for 1.5 vol.% of LPG shows as time after exposure increases, resistance increases up to

202.58 MΩ, after that it becomes constant. Further Curve R4 for 2 vol.% of LPG resistance drastically increases from 82.73 MΩ to 254.13 MΩ with time after exposure up to 350 sec respectively. In Figure 7 (b), curve R1 for 0.5 vol.% of LPG exhibits that the resistance varied 100 MΩ to 811.24 MΩ and becomes constant. Curve R2 for 1 vol.% of LPG exhibits improvement over the previous and the resistance increases from 100 MΩ to 894.86 MΩ and then it becomes constant. Curve R3 for 1.5 vol.% of LPG shows as time after exposure increases, resistance increases up to 1059.39 MΩ, After that Curve R4 for 2 vol.% of LPG resistance drastically increases from 100 MΩ to 1139.97 MΩ with time after exposure up to 300 sec respectively. This shows that the resistance increases maximum in curve R4 for 2 vol.% of LPG for (Sn-Ti)O_2 nanocomposites. Figure 8(a and b) illustrates variations in average sensitivity for pure TiO_2 and (Sn-Ti)O_2 thick film with time after exposure for different vol.% of LPG and it was found that as the concentration of LPG (in vol.%) inside the chamber increases, average sensitivity of the sensor increases linearly. The maximum average sensitivity for pure TiO_2 were found 2.4 and 3.0 for 1.5 and 2 vol.% of LPG. The maximum average sensitivity for (Sn-Ti)O_2 nanocomposites were found 10 and 11 for 1.5 and 2 vol.% of LPG. Sensor response curves are shown in Figure 9(a and b) and the maximum values of sensor responses for pure TiO_2 were 145 and 207 for 1.5 and 2 vol.% of LPG. The maximum values of sensor responses for (Sn-Ti)O_2 were 959 and 1040 for 1.5 and 2 vol.% of LPG. Response and recovery times were calculated and found 50 and 250 sec. Fig. 10(a and b) shows the reproducibility curve for 2 vol.% of LPG. Results were found reproducible within ±96% and ±97% accuracy for pure TiO_2 and (Sn-Ti)O_2 respectively.

It is clear from the above observation that LPG sensing behavior of (Sn-Ti)O_2 nanocomposite shows maximum average sensitivity for 2 vol.% of LPG as shown in Figure 11. The difference in response for pure TiO_2 and (Sn-Ti)O_2 might be recognized to adsorption of LPG and reaction between LPG and the adsorbed oxygen species. The amount of adsorbed oxygen species is fairly important for providing sufficient reactants for the reaction. As (Sn-Ti)O_2 nanocomposites surface shows more adsorption sites and exposed surface area therefore, it shows better response than the pure TiO_2.

A polycrystalline semiconductor has the structure with large number of grains and grain boundaries. In contrast to single crystalline materials, polycrystalline material gives rise to local potential barriers between the grains. The electrical properties of the surface of the thick film and surface boundaries between the grains are affected by the adsorption and desorption of gas molecules. The atmospheric oxygen molecules (O_2) are adsorbed on the surface of the (Sn-Ti)O_2 [30-31]. They capture the electrons from conduction band of the sensing material as below:

$O_{2\,(gas)} \leftrightarrow O_{2\,(ads)}$ (thick film surface)

$O_{2\,(ads)} + e^- \leftrightarrow O_2^-$ (thick film surface)

Due to this chemisorption, electronic conductivity decreases, this results an increase in the resistance of the sensing material. Thus the equilibration of the chemisorption process results in stabilization of the surface resistance. Any process that disturbs this equilibrium gives rise to change in conductance of semiconductors.

Nanocomposites based on metal oxide semiconductors are mainly used to detect small concentration of reducing and combustible gases in air. When the crystal size is decreasing, more and more surfaces is exposed. So fraction of atoms at the grain boundaries contains a high density of defects like vacancies, dangling bonds, which can play an important role in the transport properties of electrons. The mechanism that can alter the conductivity of a metal oxide gas sensor is based upon modification of the bulk resistance of the material. Often this type of change is only dependent on the partial pressure of oxygen in the atmosphere. For the sensors, the defect chemistry of the oxide is very important because the bulk of the material must equilibrate with the oxygen in the system. The change in electrical conductivity of the material has been given by the following equation-

$$\sigma \sim \sigma_0 \exp(E_a/kT)\, p(O_2)^{1/n}$$

Where σ is the electronic conductivity, E_a is the activation energy, k is the Boltzmann constant, T is the temperature, $p(O_2)$ is the partial pressure of gaseous oxygen and n is a value that depends on the nature of the point defects arising when oxygen is removed from the lattice.

Sensing performance, especially response, is controlled by three independent factors: the receptor function, transducers function and utility. Receptor function concerns the ability of the metal oxide surface to interact with the target gas. Chemical properties of the surface oxygen of the oxides are responsible for this interaction in a metal oxide semiconductor based device and this function can be largely modified. When LPG was exposed to the surface area of semiconducting oxide, then reaction takes place between LPG and oxygen molecules, which was adsorbed by the TiO_2 and (Sn-Ti)O_2 nanocomposite. As LPG was able to react with the adsorbed oxygen then the combustion products such as water depart, and a potential barrier to charge transport would be developed i.e., this mechanism involves the displacement of adsorbed oxygen species by formation of water [32-33]. This can be understood by following reaction:

$$C_nH_{2n+2} + 2O_2^- \longrightarrow C_nH_{2n}O + 2H_2O + 2e^-$$

where C_nH_{2n+2} represents the various hydrocarbons.

These liberated electrons recombine with the majority carriers (holes) of sensing films resulting in a decrease of conductivity. The formation of barrier was due to reduction in the concentration of charge carriers and thereby, result was

an increase in resistance of the sensing element with time. As the pressure of the gas inside the chamber was increased, the rate of the formation of such product increases and potential barrier to charge transport becomes stronger which has stopped the further formation constituting the resistance constant [34].

The resistance variation of the (Sn-Ti)O_2 with temperature can be described through typical band conduction. It can be noted that a change in temperature will alter the resistance because both the charge of the surface species (O_2, O_2^-, O^- or O^{2-}) as well as their coverage can be altered in this process. Since the conduction process in metal oxide semiconducting materials can depend heavily on grain boundaries, therefore large and small particle sizes of material are responsible for deviation from the linear characteristic. In the overall conduction process a contribution arising from the participation of tin titanate nanocomposites with lower average particle size and another with higher average particle size i.e., the distribution of particle size dominates in thermally activated conduction process in the case of (Sn-Ti)O_2 nanocomposite. The energy transition during the investigation in the temperature range 150-230 ºC which may be an electron excitation from valence band to an acceptor level creates a hole in valence band for conduction. Therefore this transition controls the R-T characteristics. As activation energy measures the thermal or other form of energy required to raise electrons from the donor levels to the conduction band or to accept electrons by the acceptor levels from the valence band. As the interaction probability of sensing element with LPG is given by the Boltzman factor exp(-E_a/kT). Therefore for the higher probability of interaction to occur, E_a should be least for room temperature LPG sensor. This small value of activation energy (0.398 eV) is significant for the detection of LPG at room temperature.

Conclusion

This work demonstrated the successful preparation of pure TiO_2 and (Sn-Ti)O_2 nanocomposite using soft chemical route at room temperature. The value of average sensitivity for pure TiO_2 and (Sn-Ti)O_2 nanocomposite were 3.0 and 11 respectively for 2 vol.% of LPG. The variation in the sensing property has followed to the morphology of the particles. SEM image clearly shows that the surface of (Sn-Ti)O_2 nanocomposite is more porous than the pure TiO_2 surface. A bunch like morphology has been disappeared as in pure TiO_2 and LPG interacts better with that type of morphology. Thus the experimental results demonstrate that (Sn-Ti)O_2 nanocomposite appears to be a promising material for the LPG sensing than nano-sized pure TiO_2.

References

1. E. Regis, Little Brown and Company, Boston **(1995)**.
2. X. Liu, X.H. Wu, H. Cao and R.P.H. Chang, J. Appl. Phys. 95, 3141 **(2004)**.
3. D.H. Zhang, C. Li, S. Han, et al., Appl. Phys. Lett. 82, 112 **(2003)**.
4. J.W. ollenstein, M. Burgmair, G. Plescher, et al., Sensors and Actuators B 93, 448 **(2003)**.
5. J. Xu, Q. Pan, Y. Shun, and Z. Tian Sensors and Actuators *B* 66, 277 **(20002)**.
6. P. Bhattacharyya, P. K. Basu, C. Lang, H. Saha, and S. Basu, Sensors and Actuators B 129, 551 **(2008)**.
7. T. Anderson, F. Ren, S. Pearton, B.S. Kang, H.T. Wang, C. Y. Chang and Lin, Sensors 9, 4669 (**2009)**.
8. Y. Vashpanov, H. Choo and D.S. Kim, Sensors 11, 10930 (**2011)**.
9. R. B. Waghulade, R. Pasricha and P. P. Patil, Talanta 72, 594 **(2007)**.
10. M.V. Vaishampayan, R.G. Deshmukh and I.S. Mulla, Sensors and Actuators B 131, 665 **(2008)**.
11. V. R. Shinde, T. P. Gujar, and C. D. Lokhande, Sensors and Actuators B 123, 701 **(2007)**.
12. Liang-Dong Feng, Xing-Jiu Huang and Yang-Kyu Choi, Microchim Acta 156, 245 **(2007)**.
13. L.A. Patil, M.D. Shinde, A.R. Bari, V.V. Deo, D.M. Patil and M.P. Kaushik, Sensors and Actuators B 155, 174 **(2011)**.
14. S.K. Omanwar and Tripti Shukla Sensors Letters 12, 1 **(2014)**.
15. Tripti Shukla Journal of Sensor Technology 2, 102 **(2012)**.
16. M. S. Wagh, G. H. Jain, D. R. Patil, S. A. Patil and L. A. Patil, Sensors and Actuators B 115, 128 **(2006)**.
17. B. C. Yadav, Satyendra Singh, Anuradha Yadav and Tripti Shukla International Journal of Nanoscience 10, 1 **(2011)**.
18. D.N. Huyen, N.T. Tung, N.D. Thien, L.H. Thanh, Sensors 11, 1924 **(2011)**.
19. A. B. Bodade, M. Alvi, A.V. Kadu, S. V. Jagtap, S. K. Rithe, P. R. Padole and G. N. Chaudhari Sensors & Transducers 98, 6 **(2008)**.
20. X. Chen, W. Lu, W. Zhu, S. Y. Lim, and S. A. Akbar, Surface and Coatings Technology, 167, 203 **(2003)**.
21. M. S. Wagh, G. H. Jain, D. R. Patil, S. A. Patil and L. A. Patil, Sensors and Actuators B 115, 128 **(2006)**.

22. S.A. Patil, L.A. Patil , D.R. Patil, G.H. Jain and M.S. Wagh, Sensors and Actuators B 123, 233 **(2007)**.
23. R. H. Bari and S. B. Patil, International Journal of Techno Chem Research 01, 86 **(2015)**.
24. L. Zbroniec, A. Martucci, T. Sasakil and N. Koshizaki, Appl. Phys. A 79, 1303 **(2004)**.
25. M.V. Vaishampayan, R.G. Deshmukh and I.S. Mulla, Sensors and Actuators B 131, 665 **(2008)**.
26. G.H. Jain, L.A. Patil, M.S. Wagh, D.R. Patil, S.A. Patil, Sensors and Actuators B 117, 159 **(2006)**.
27. C.V. Gopal Reddy, W. Cao, O.K. Tan, W. Zhu and S.A. Akbar, Sensors and Actuators B 94,99 **(2003)**.
28. M.C. Carotta, A. Cervia, S. Gherardi, V. Guidia, C. Malagu, G. Martinellia, B. Vendemiatia, M. Sacerdoti, G. Ghiotti, S. Morandic, S. Lettieri, P. Maddalenad and A. Setaro, Sensors and Actuators B 139 329 **(2009)**.
29. Tripti Shukla, B. C. Yadav, and Poonam Tandon Sensor Letters 9, 1 **(2011).**
30. W.J. Moon, J.H. Yu and G.M. Choi, Journal of Electroceramics 13 707 **(2004)**.
31. P.T. Moseley, Sensors and Actuators B 6 149 **(1992)**.
32. N. Yamazoe, Sensors and Actuators B 108, 2 **(2005)**.
33. S**.** Basu and P.K. Basu, Nanocrystalline Metal Oxides for Methane Sensors: Role of Noble Metals, Journal of Sensors 861968 1-20 **(2009)**.

ISSN 2347-3487

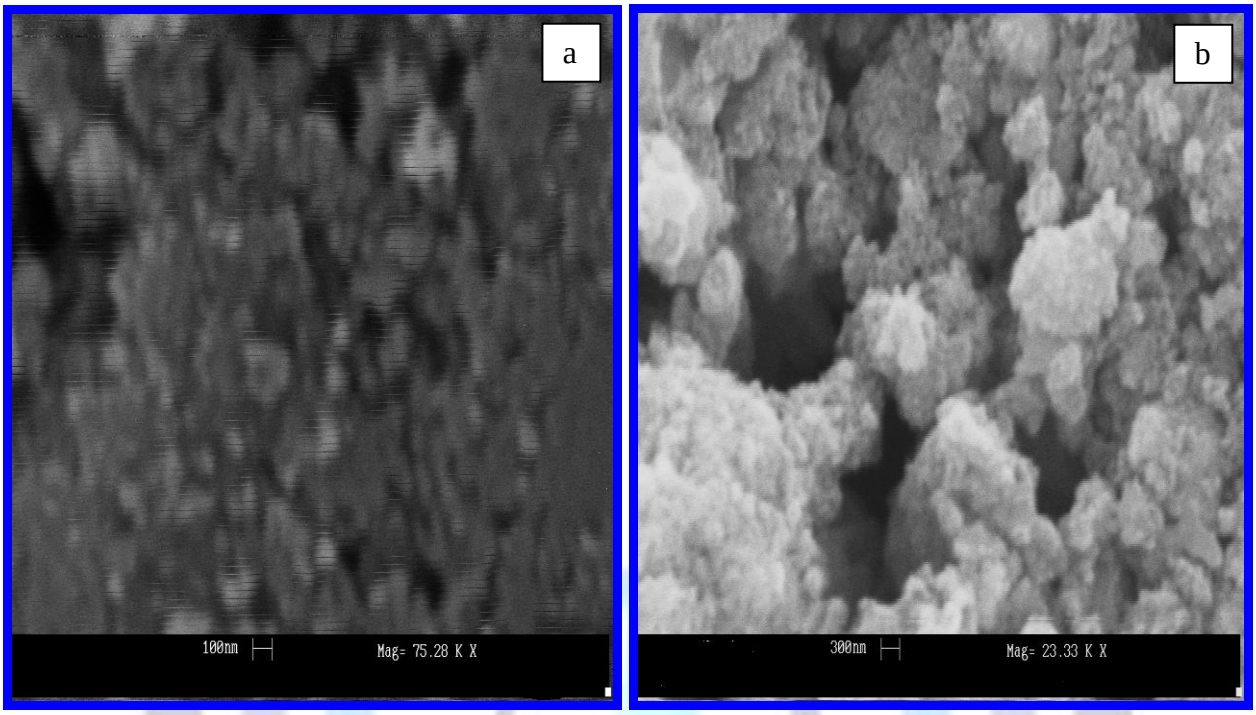

Figure 1 SEM at nanoscale (a) for pure TiO_2 (b) for $(Sn\text{-}Ti)O_2$

ISSN 2347-3487

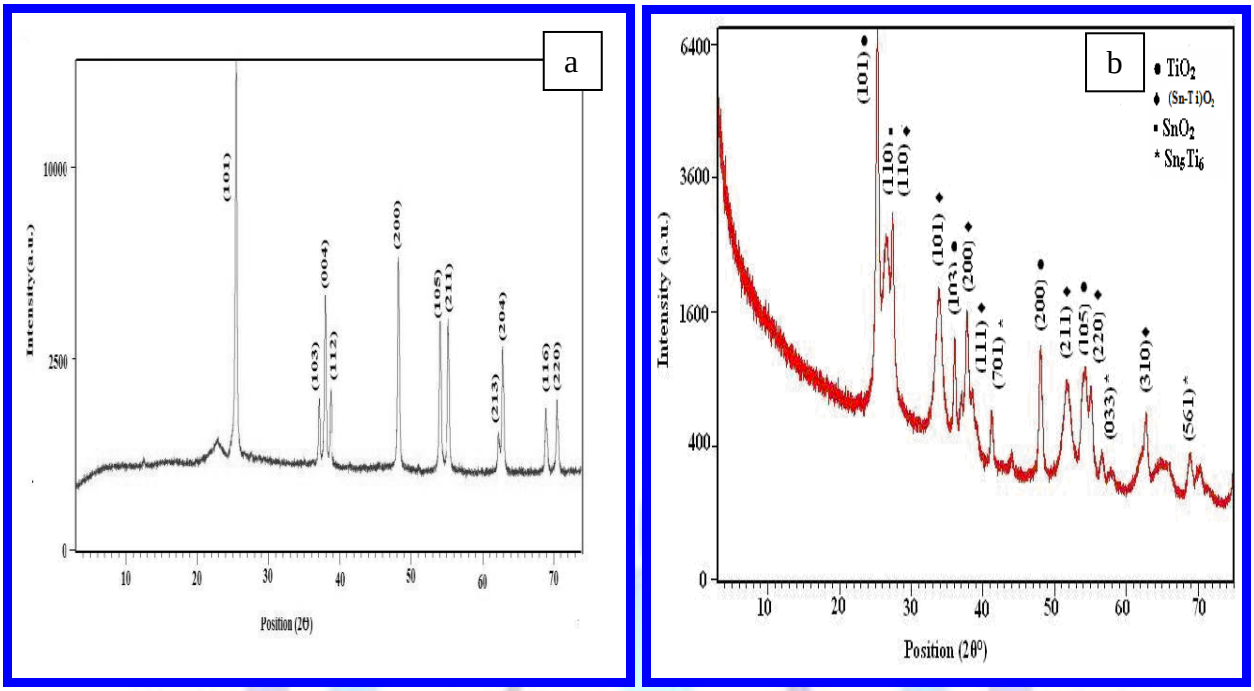

Figure 2 X- Ray Diffraction in the form of Powder (a) for pure TiO_2 (b) for $(Sn-Ti)O_2$

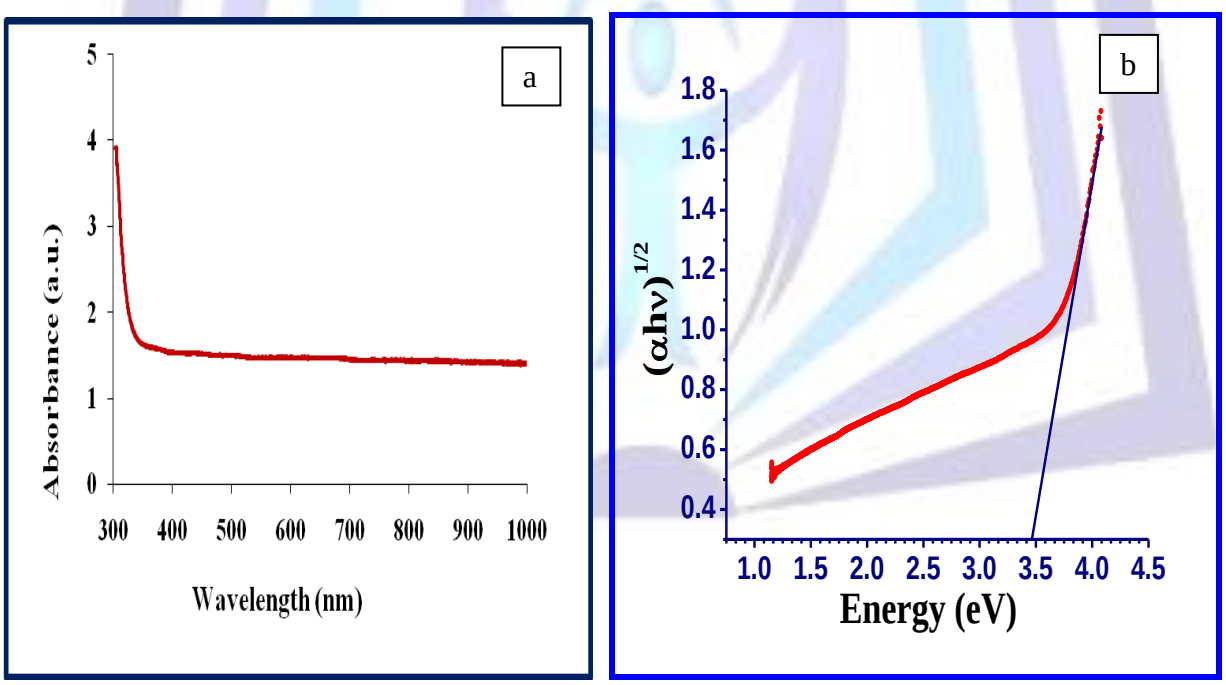

Figure 3 (a) UV-Visible absorption spectra of pure TiO_2 (b) Tauc plot for optical energy gap.

ISSN 2347-3487

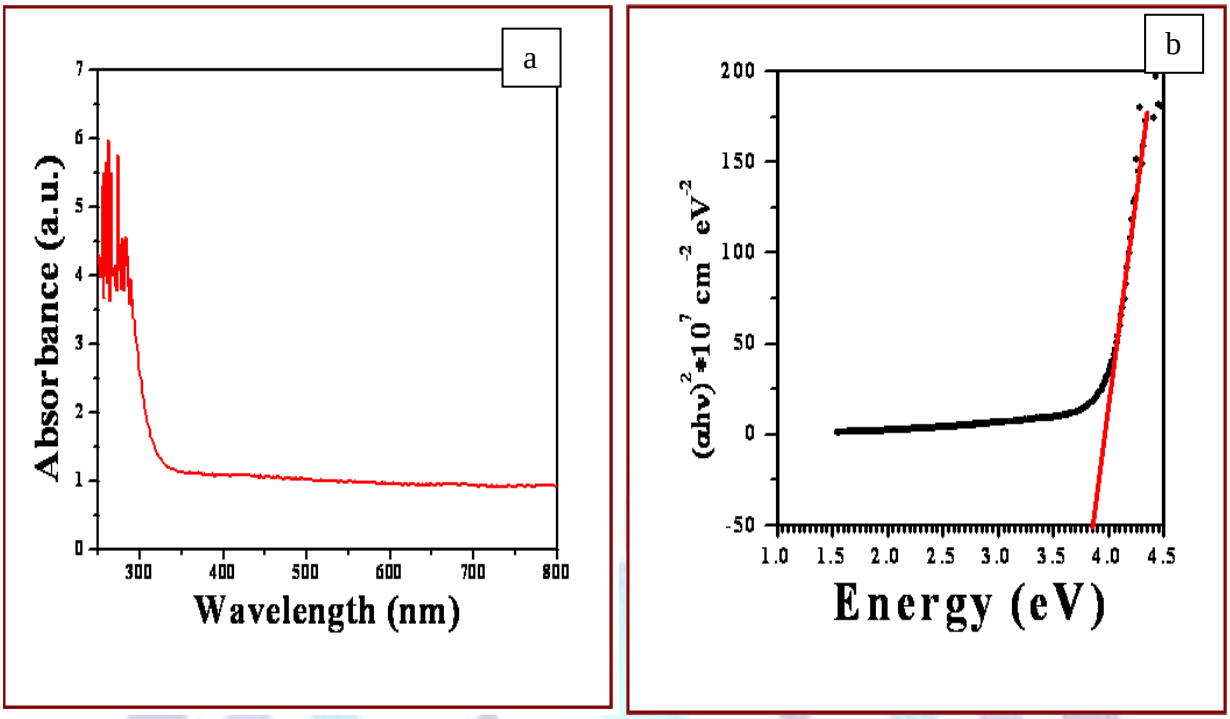

Figure 4 (a) UV-Visible absorption spectra of (Sn-Ti)O_2 (b) Tauc plot for optical energy gap.

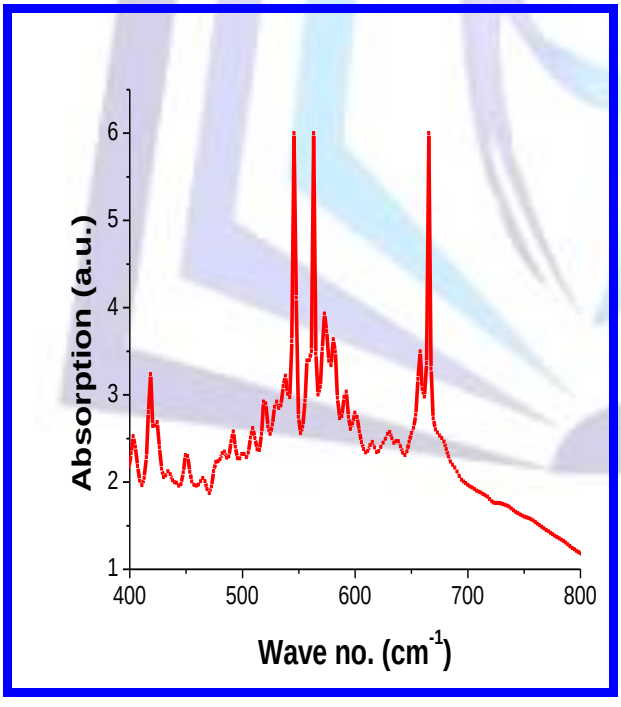

Figure 5 FTIR spectra of (Sn-Ti)O_2 nanocomposites

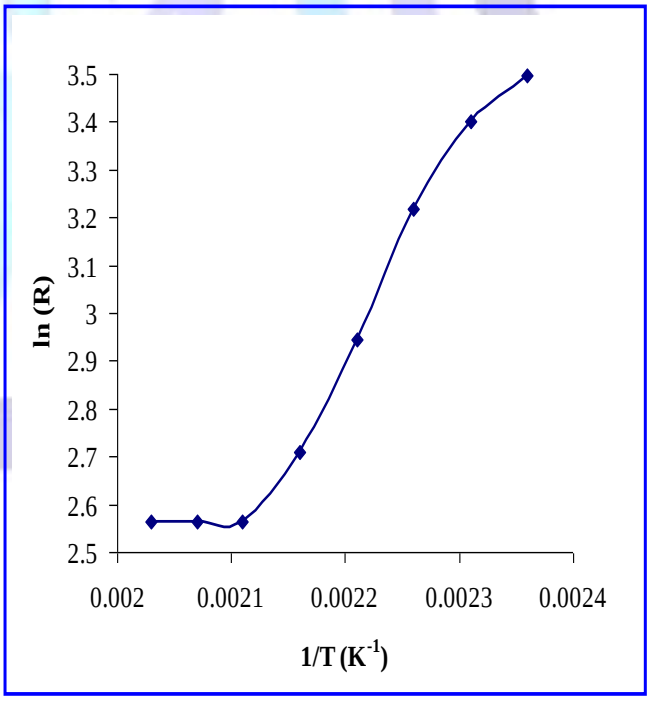

Figure 6 Arrhenius plot of (Sn-Ti)O_2 nanocomposites

ISSN 2347-3487

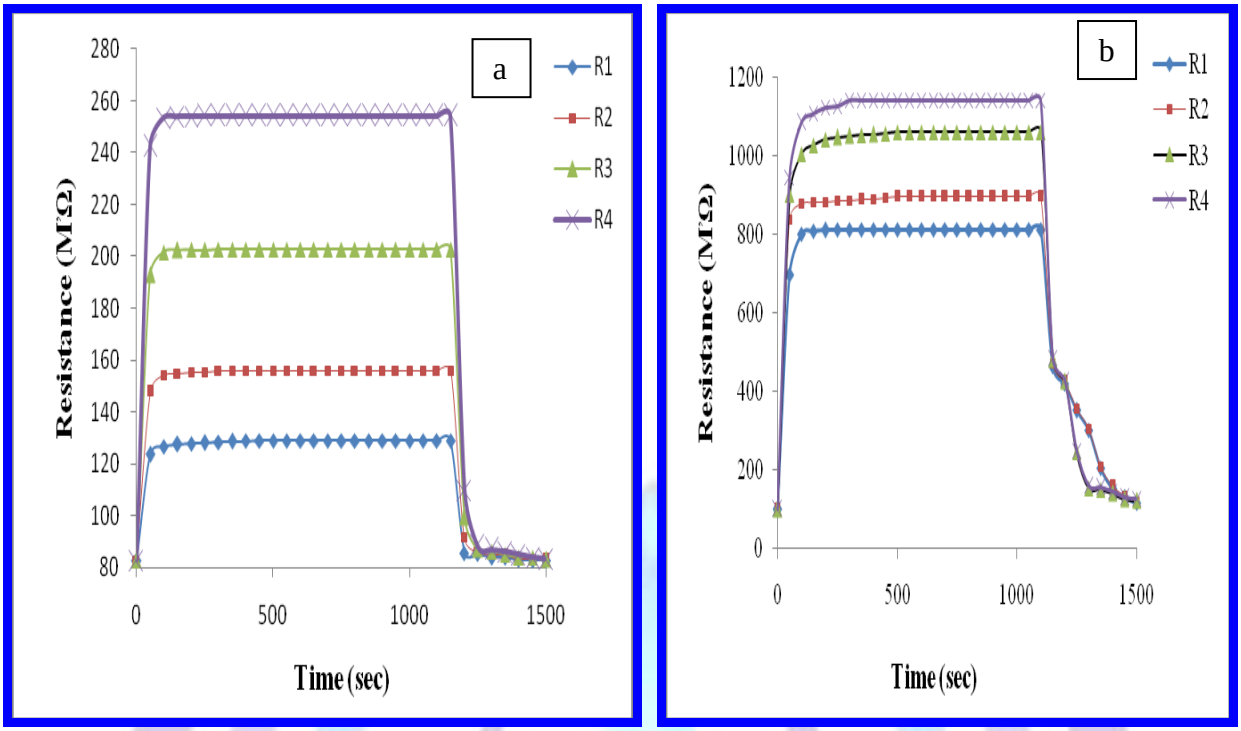

Figure 7 Variations of resistance with time after exposure for different vol.% of LPG (a) for pure TiO_2 (b) for (Sn-Ti)O_2 nanocomposites

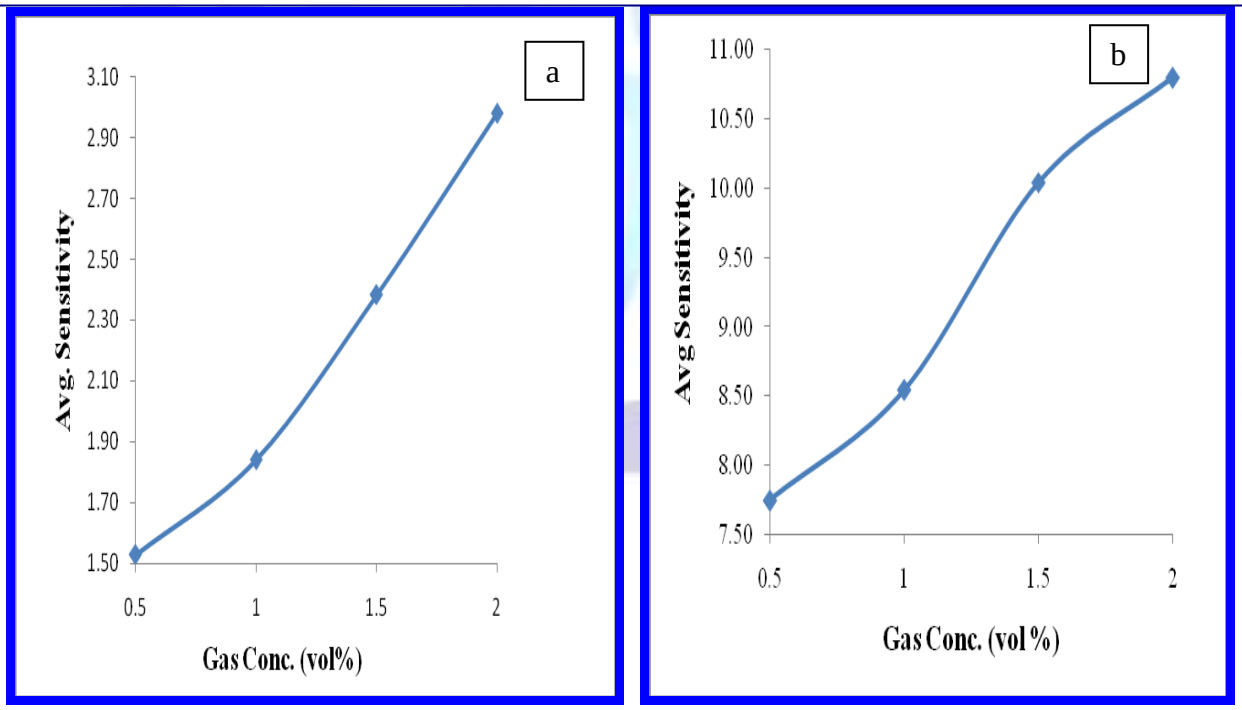

Figure 8 Avg Sensitivity curves of for different vol.% of LPG (a) for pure TiO_2 (b) for (Sn-Ti)O_2 nanocomposites

ISSN 2347-3487

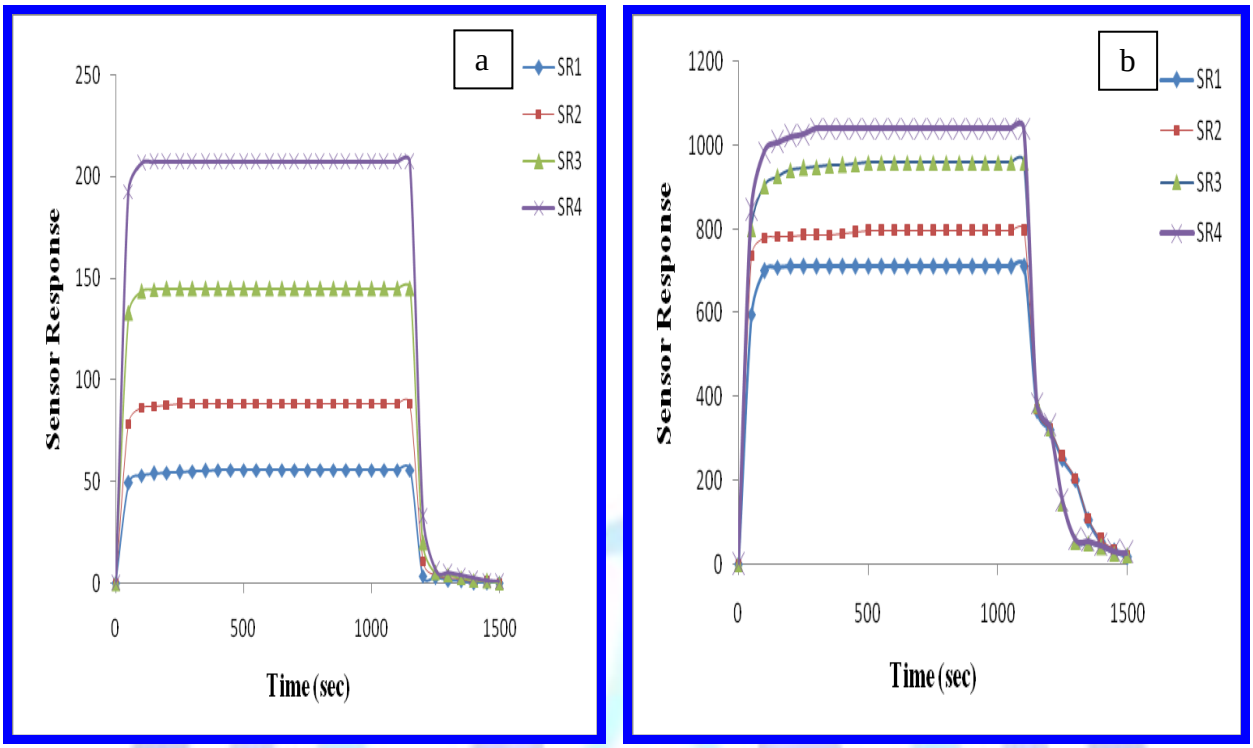

Figure 9 Sensor Response curves of sensing materials with time after exposure for different vol.% of LPG (a) for pure TiO_2 (b) for (Sn-Ti)O_2 nanocomposites

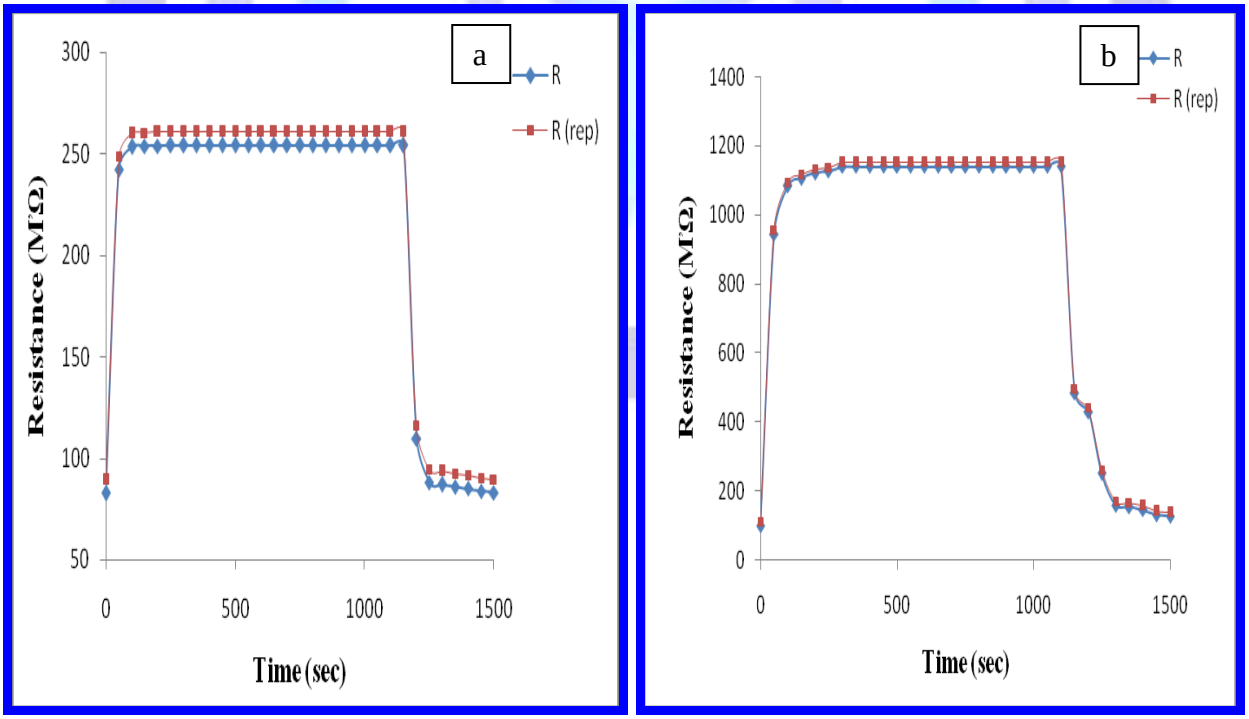

Figure 10 Reproducibility curves (a) for pure TiO_2 (b) for (Sn-Ti)O_2 nanocomposites

ISSN 2347-3487

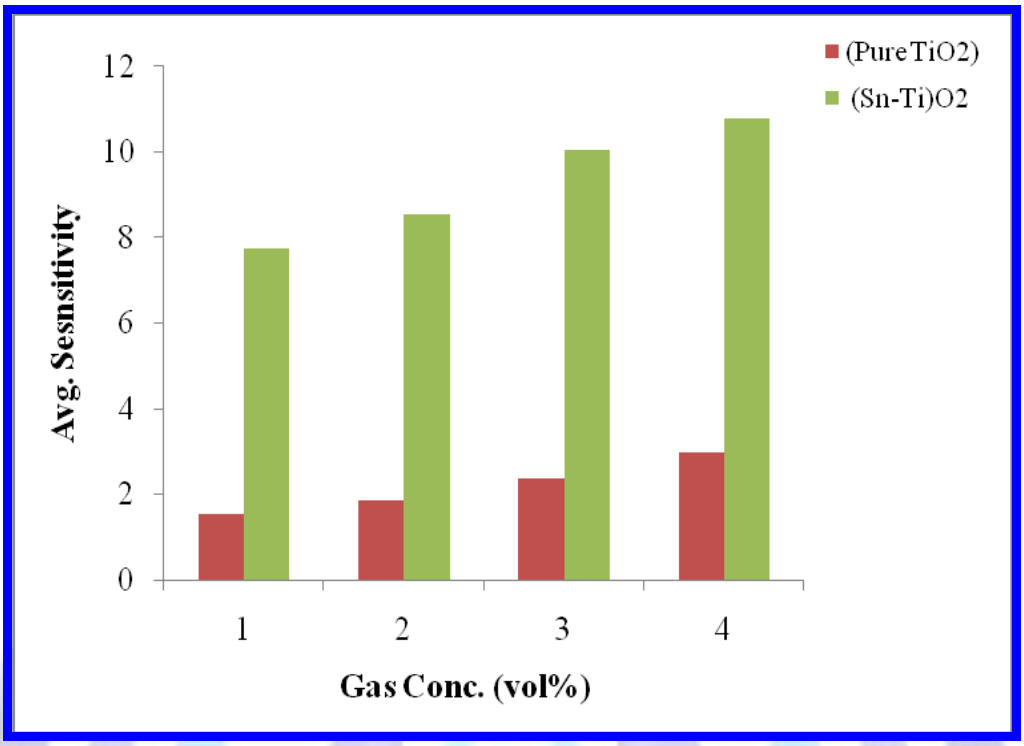

Figure 9 Comparative Avg. Sensitivity curves for pure TiO_2 and (Sn-Ti)O_2 nanocomposites with time after exposure for different vol.% of LPG.

Tripti Shukla

Miss Tripti Shukla has received her B.Sc. degree in 2004 from Lucknow University and M.Sc. degree in 2007 from Dr. RML Awadh University, Faizabad Uttar Pradesh, India. Presently she is pursuing her research work from Sant Gadge Baba Amravati University, Amravati, M.S. India. Her current interests of research are in the area of synthesis and characterization of metal oxide based nanocomposites and their application as a LPG sensor.

Prof. Dr. S. K. Omanwar

Prof. Dr. S. K. Omanwar is working as Head of the department, Department of Physics, Sant Gadge Baba Amravati University, Amravati. He is having more than 24 years of teaching and research experience. He has more than 400 research and review article in various national and international journals. He has guided 24 PhD. students and having 2 research patients.